Field dependent study on the impact of co-evaporated multihits and ion pile-up for the apparent stoichiometric quantification of GaN and AlN

Richard J. H. Morris[1], Ramya Cuduvally[1,2], Jhao-Rong Lin[1], Ming Zhao[1], Wilfried Vandervorst[1,2], Mattias Thuvander[3], Claudia Fleischmann[1,2].

Corresponding Author: richard.morris@imec.be

[1.] IMEC, Kapeldreef 75, 3001, Leuven, Belgium.

[2.] Quantum Solid State Physics (QSP), KU Leuven, Celestijnenlaan 220D, 3001, Leuven, Belgium.

3. Chalmers University of Technology, Göteborg, Sweden.

Abstract

For atom probe tomography, multihits and any associated ion pile-up are viewed as an "Achilles" heel when trying to establish accurate stoichiometric quantification. A significant reason for multihits and ion pile-up is credited to co-evaporation events. The impact is the underestimation of one or more elements present due to detector inadequacies when the field evaporated ions are spatially and temporally close. Nitride materials, especially GaN and AlN, have been shown to suffer a strong field dependent compositional bias, with N having the characteristics for being a species prone to ion pile-up. In this paper we have explored through field dependent measurements on GaN and AlN the associated impact of co-evaporated multihits and ion pile-up. To achieve this a normal CAMECA electrode along with a specially modified GRID electrode, which was designed to manipulate co-evaporated ions and hence ion pile-up, were employed. From our results and in-depth analysis, any co-evaporation and associated ion pile-up is found to be either very small, or not species dependent. Thus, ion pile-up cannot be attributed as the cause for the significant N underestimation observed in these materials.

public

Introduction

In the discipline of Atom Probe Tomography (APT), reproducible and accurate stoichiometric quantification remains a challenge. As was highlighted recently by Cuduvally *et al.* [1], there are many possible causes underpinning this, with multihits and the potential for ion pile-up being among a list of reasons for compositional bias issues. Multihits have formed the topic of many APT studies [2, 3, 4, 5, 6] and arise when many ions are simultaneously emitted from the specimen tip and arrive at the detector together. In theory, the detection and correct mass assignment of multihits should not result in a compositional bias. However, the concern surrounding multihits for the APT community involves those that we do not detect, an effect termed "ion pile-up" [2, 5, 6]. Ion pile-up is a limitation in the detector technology, i.e., arising from the dead-time and dead-zone [5, 6]. Given these known limitations, there have been various attempts to improve the APT detector systems through hardware improvements, e.g., advanced delay line detectors and the analysis electronics [5, 7, 8, 9, 10], and via the software, i.e., algorithms applied to the signals generated from the hardware [7, 8, 9]. A reason given for multihit ion pile-up is co-evaporation, i.e., as one atom is field evaporated it exposes its neighboring atom(s), which then experience an enhanced field leading to an increased probability for a same pulse evaporation event [11]. These co-evaporated ions then arrive at the detector with an insufficient spatial separation to all be counted.

The number of multihits detected is correlated with the material properties under investigation. Elements that possess a higher field of evaporation (FOE) typically register a larger number of multihits [5, 12]. Intuitively, one might therefore infer that the more multihits present, the higher the probability for ion pile-up, but to the best of the authors' knowledge, there is currently no evidence to support this hypothesis. For heterogenous samples where the FOE

public

between the constituent species varies significantly, it has also been proposed that compositional bias effects arise from a larger loss of one species through ion pile-up [5]. A potential mechanism proposed in support of this is that the element with the higher FOE is retained on the sample surface. This element may then migrate towards a higher field emission region where it forms a cluster which is easier to ionize but also has the potential to dissociate. Alternatively, when a lower field element adjoining is removed, the higher FOE element becomes isolated on the surface leading to an enhanced localized field and its subsequent co-evaporated emission [13].

A few examples within the literature where the aforementioned effects are attributed to compositional analysis bias include the work of Meisenkothen *et al.* [6] who concluded that the underestimation of B in Si was related to the number of multihits in their study; Tu *et al.* [14] who also proposed B multihits in the form of a burst evaporation was the cause of their B compositional discrepancies for certain conditions; and Martin *et al*. [15] who concluded that the differences in cluster stoichiometry between instruments was linked to the different multihit capabilities of the two instruments used in their study. Another material system where ion-pile up is believed to significantly influence the stoichiometric quantification is for carbon in tungsten carbide and carbides in steels [3]. To investigate this further, Thuvander *et al*. [3] modified a Local Electrode Atom Probe (LEAP) electrode by adding a grid to its reverse side. This electrode will now be referred to as the GRID electrode. The principle behind the GRID electrode was to intentionally decrease the detection efficiency in a controlled manner by deliberately blocking co-evaporated ions from reaching the detector [3]. Thus, if one species were to preferentially co-evaporate leading to ion pile-up, i.e., resulting in some of this species not being detected, then the impact of inserting the GRID electrode would be to reduce the detection of spatially and temporally correlated co-evaporated ions. This also includes any mixed ions that were previously detected. This has the

public

effect of equalizing out the ion pile-up between all species. However, the results presented to date are limited and have been somewhat mixed with certain studies claiming some evidence for a multihit/ion pile-up stoichiometry dependence for carbon rich clusters within steels, however, for a homogenous tungsten carbide sample, the effect appeared to be less prevalent [3].

Another parameter that impacts material stoichiometric quantification is the analysis conditions. Numerous studies have now demonstrated that for different apex fields, a change in the apparent stoichiometric quantification for the same sample can occur [16, 17, 18, 19]. Additionally, the number of multihits detected have also been shown to have an apex field dependence [19]. For the tungsten carbide [3], carbon clusters in steels [3], and the B in Si [6, 14] examples previously mentioned, the apex field (either the average or local apex field at the cluster emission site or crystal structure pole and zone lines), was not reported and so any correlation between the analysis conditions and potential ion pile-up cannot be taken into consideration.

In this paper, the correlation between apex field and multihit ion pile-up as a potential reason for the compositional bias observed for GaN and AlN has been explored. GaN and AlN were chosen because of their growing importance within the semiconductor device technology field and that they have both shown considerable compositional bias as a function of the apex field [16, 17, 18, 19]. Electric field dependent measurements on these samples using a LEAP 5000 XR fitted with a standard CAMECA electrode and a specially modified GRID electrode [3] to remove co-evaporated ions were performed. Although the insertion of the GRID electrode was found to significantly reduce the number of multihits, and an in-depth look at same isotope same charge state (SISCS) and mixed ions (different mass and mass-to charge ratio) double hits showed some evidence of spatial/temporal co-evaporated ion emission that can lead to ion pile-up, the apparent stoichiometry remained unchanged. Our findings therefore do not support ion pile-up as the

public

primary loss mechanism leading to the field dependent compositional bias observed for GaN and AlN.

Experimental

For this study, GaN and AlN bulk layers grown using the metalorganic chemical vapor deposition (MOCVD) technique [20] were studied. Based on the charge neutrality consideration, there was no reason to presume anything other than a stoichiometry of 50:50 in both cases. All the APT sample tips used in this study were prepared using the conventional focused ion beam (FIB) lift-out approach [21] with an FEI Helios 450 FIB/SEM. The final tip diameter for all the samples was in the range of 50 - 100 nm, and a 2 kV (10 pA) Ga beam clean prior to loading into the atom probe was adopted. The atom probe analysis was conducted on a LEAP 5000 XR in laser mode (λ = 355 nm). A base temperature of 50 K; a pulse frequency of 125 kHz; and a voltage reconstruction were used. The field dependent measurements were performed by keeping the detection rate fixed and varying the laser pulse energy (LPE). As the LPE applied was different depending upon the material and electrode type employed, the values applied will be reported alongside the results.

A normal local electrode (NE) supplied by CAMECA and a modified CAMECA electrode that incorporated a GRID [3] mounted on the electrode underside were used. The detection rate for the NE analysis was 0.5%, while for the GRID electrode this was reduced to 0.1% to try and maintain a similar apex evaporation rate between the two electrode experiments. The reason for doing this was to compensate for the different detection efficiencies (detection efficiency of ~52% for the normal electrode and ~7.3% for the GRID electrode). The determination of the apparent elemental concentrations for all the samples was performed using the CAMECA IVAS 3.8 software by ranging the peaks in the mass spectrum. CAMECA's TaP3D software was also used

public

for the extraction of single and multi-hit information, while in-house MATLAB codes were used to extract the double hit per pulse event information.

Results and discussion

1. GaN

Figures 1 (a) and (b) show the mass spectra for the GaN samples measured using (a) the CAMECA NE and (b) the GRID electrode. Both these spectra have the same mass peaks present and are highly representative of what was observed for all the conditions used in this part of the study. From the mass spectra it is seen that the largest ion emission, and therefore influence on the determined stoichiometry, arises from $^{14}N^{++}$, $^{14}N^{+}$, $^{14}N_2^{+}$, $^{69}Ga^{+}$, $^{69}Ga^{++}$, $^{71}Ga^{+}$ and $^{71}Ga^{++}$.

Based on Kingham's post ionization theory [22], the charge state ratio (CSR) of an element present can be used as an indication for the average apex field and has been demonstrated to offer a reliable approach for comparing analysis between samples of the same stoichiometry [16, 18, 19]. Both mass spectra presented in Figure 1 were collected for a similar apex field as given by the average Ga CSR, i.e. $\frac{Ga^{++}}{Ga^{+}} = 0.330 \pm 0.001$ for the NE and $\frac{Ga^{++}}{Ga^{+}} = 0.341 \pm 0.001$ for the GRID electrode, reflecting the slightly higher effective evaporation rate used for the latter. The apparent stoichiometry determined (and noting that 14 Da was assigned as $^{14}N^{+}$) for these two analyses were also found to be in good agreement, with the NE data yielding Ga = 48.8 ± 0.1 at.% and N = 51.2 ± 0.1 at.%; while for the GRID we found Ga = 50.5 ± 0.1 at.% and N = 49.5 ± 0.1 at.%. We note that the errors quoted are just the 1σ counting statistics [*23*].

public

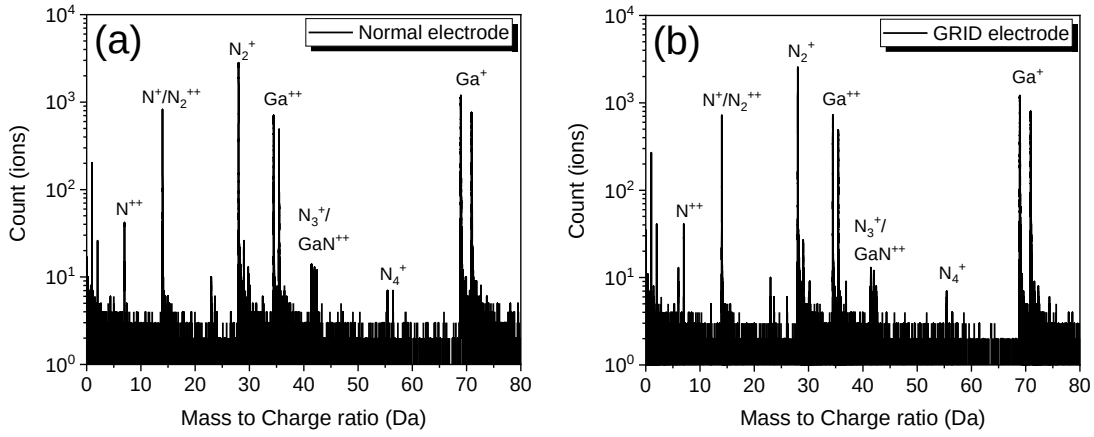

Figure 1. Mass spectra taken from GaN using (a) the CAMECA NE and (b) the GRID electrode.

From an electric field dependent study, the apparent stoichiometry of the GaN sample as a function of the Ga CSR for both the NE and GRID electrode was determined and is shown in Figure 2 (a).

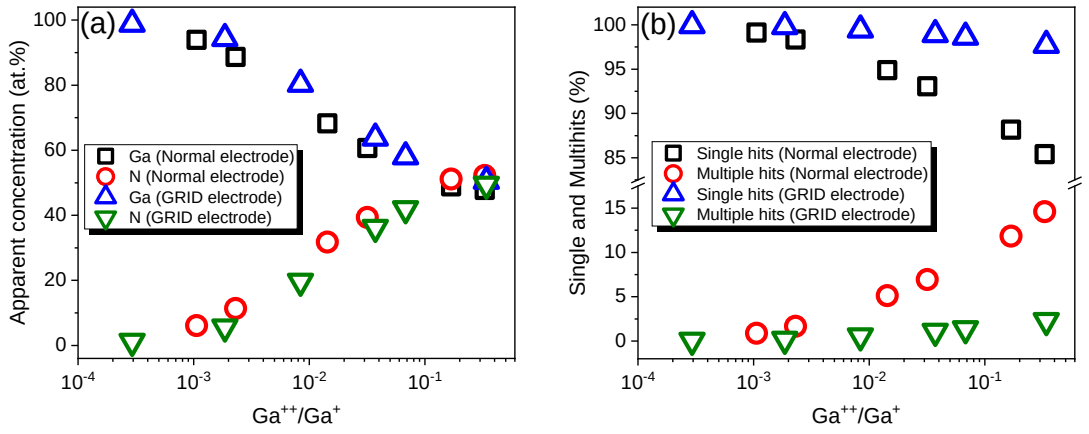

Figure 2. (a) Plot of the apparent Ga and N stoichiometry as a function of Ga CSR and (b) Single and multihits as a function of Ga CSR for the same data set.

public

For each data point on this plot, ~500,000 atoms were collected. For the NE experiments the LPE was varied between 20 - 0.005 pJ while for the GRID electrode it ranged between 20 – 0.01 pJ. The apparent Ga and N stoichiometry determined as a function of the Ga CSR, i.e., average apex field, for both electrodes were found to be in good agreement. Moreover, the findings are in excellent agreement with those previously reported for GaN measured using a CAMECA NE in the LEAP 5000 XR or the LAWATAP [18, 19], again demonstrating the high reproducibility of the analysis and CSR comparison approach for this material system.

As the multi-hit influence on the stoichiometry was a focus of this study, then, to investigate this further the number of single- and multihits detected for the same electric field dependent data (Figure 2a) was extracted and is presented in Figure 2b. For the lower apex field range, i.e., $\left(\frac{Ga^{++}}{Ga^{+}} \leq \sim 2 \times 10^{-3}\right)$, the ratio between single to multihits for both electrodes are found to be similar i.e., ~96% single hits and ~ 4% multihits. The number of multihits are observed to increase with increasing Ga CSR, i.e., apex field, for both electrode types. However, the rate of increase significantly diverges with the NE showing a larger increase for the same apex field. Even with this large divergence in multihits as a function of apex field between the two electrode types, the apparent stoichiometry as a function of apex field (Figure 2(a)) remains the same.

public

From the same data set, the maximum number of ions per pulse detected as function of Ga CSR for both the NE and GRID electrode were determined and are presented in Figure 3. A potential consequence of multihits is detector saturation i.e., this occurs when many ions per pulse arrive too close together at the detector with too small a difference in their flight time to all be counted. If this occurs, the multiples will be undercounted. This could also result in a preferential underestimation if only certain species present were more prone to this effect. However, improvements to help counteract this have been made, with up to 15 ions per pulse specified in the LEAP product description [24] while 30 ions per pulse have been reported in the literature where improvements in the timing information extraction and digitization of the analogue signal processing [5]. As such, the maximum number of hits per pulse of 9 observed in our work for the NE is believed to be well within the current instrument capabilities.

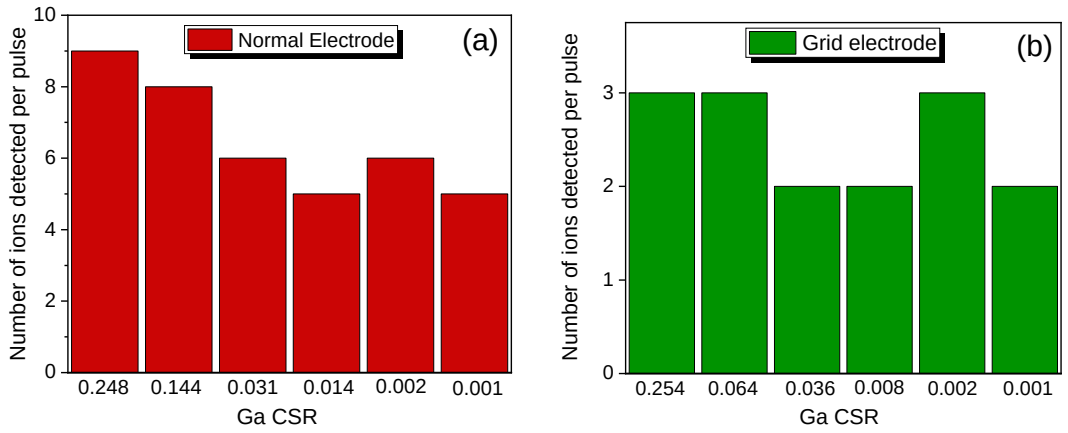

Figure 3. Plot showing the maximum number of ions per pulse as a function of Ga CSR (apex field) for the NE and GRID using the same data as figure 2.

The reduction in the number of recorded hits per pulse found for the GRID electrode as compared to the NE agrees with that previously reported by Thuvander [3]. Moreover, it also

public

follows the expected behaviour where the lower the detection efficiency the fewer multiple hits detected [3]. As the apex field was lowered there is some evidence that the number of hits per pulse decreases for the NE (drops to ~5 counts per pulse). At higher field, more ions have a probability of field-evaporating on a given pulse, so therefore we can get up to 9 at high field. For the GRID electrode the ions per pulse as a function of CSR remained almost invariant. This invariance with apex field (~3 counts per pulse) is believed to be a consequence of the number of multiples generated, which should be the same with apex field regardless of electrode used, and the lower detection efficiency of the GRID electrode. This is further supported by similar data extracted for AlN and presented later in the paper. Here the AlN shows a similar level of counts per pulse for the NE, while for the GRID electrode it again remains invariant with apex field and is limited to ~3 ion per pulse.

Other effects to consider include the constituent elements field of evaporation (FOE) and their potential to form same isotope same charge state (SISCS) ions. As previously outlined, if a large FOE difference between the constituent species of a sample exists, then preferential retention of the higher FOE species followed by its co/burst-evaporation may occur leading to ion pile-up [13]. If this were the case for GaN, the apparent stoichiometric behavior as a function of apex field would suggest N was the element with a higher FOE. The FOE for Ga (based on pure Ga) is reported to be 15 V/nm [25] while there are no reported FOE values for N in the literature. Using Müller's image hump model and Equation 1 [26] to derive the energy barrier at zero field, both the Ga and N FOE values for a GaN matrix were estimated.

$$Q_{0(\text{Ga/N in GaN})} = \frac{1}{2} E_{\text{cohesive (GaN)}} + E_{\text{ionization (Ga/N)}} - \varphi_{e\ (\text{GaN})} \qquad (1)$$

Where $Q_{0(\text{Ga/N in GaN})}$ is the Ga or N energy barrier at zero field, $E_{\text{cohesive (GaN)}}$ the cohesive energy of GaN [27], $E_{\text{ionisation (Ga/N)}}$ the ionization energies for Ga or N [25], and φ_e the surface work

public

function of GaN [28]. The N and Ga FOE values were estimated to be ~122 V/nm and ~15 V/nm respectively. These values support the hypothesis of N being the species most likely to be retained on the surface.

Same isotope co-evaporation could also affect the composition because co-evaporation of SISCS ions are expected to be more prone to ion pile-up compared to mixed isotope ions as their spatial and temporal arrival on the detector will be too small for them to all be detected. The probability of co-evaporating a same isotope Ga from GaN is smaller than that for N. This is because of the isotopic ratio difference between the elements, i.e., ^{69}Ga:^{71}Ga being 60.1:39.9 compared to ^{14}N:^{15}N which is 99.6:0.4%. To a good approximation N can be considered a monoisotopic element. Thus, any SISCS co-evaporated N, i.e., N or N_2, will be predominately formed from ^{14}N while for Ga there will be more co-evaporated ions of mixed isotope, i.e., $^{69/71}$Ga ions, which should be detected.

By inserting the GRID electrode, its influence is to reduce the detection of any co-evaporated ions that are spatially close, i.e., arise from adjoining atoms. Thus, any mixed isotope co-evaporated ions e.g., $^{69/71}Ga^{+/++}$, that arrive closely on the detector and would previously have been detected when using the NE will now be reduced, while any SISCS ions that were previously not counted due to ion pile-up remains unchanged. As discussed, if ion pile-up from SISCS ions were the issue, and it was more pronounced for one species compared to another, then the GRID electrode should have a noticeable impact. For example, as indicated above, N is the element most likely to be retained on the surface and have an increased potential for burst evaporation. Additionally, as it can be almost assumed monoisotopic it will be more prone to SISCS emission compared to Ga. Thus, N could be expected to be the element to suffer ion-pile up most. By using the GRID electrode, a reduction in any previously detected co-evaporated mixed ions, i.e., Ga,

public

would occur. However, insertion of the GRID electrode did not have a significant impact upon the apparent stoichiometry compared to the NE, indicating little to no significant preferential element co-evaporated ion pile-up is occurring.

Given the results presented above do not appear to support ion pile-up as having a significant influence on the stoichiometric variance with apex field, a further and more in-depth study into the detected number of SISCS and mixed ions, i.e., ions with dissimilar mass or mass-to-charge, using both the NE and GRID was performed. The aim was to try and elucidate how the ions are field evaporating from the apex. To extract the number and type of double hit ions per pulse recorded, in-house MATLAB codes were employed. We also focused on double ion combinations which included $^{69\,\&\,71}Ga^{+/++}$, $^{14}N^{+/++}$, and $^{14}N_2^{+}$ because these were the most significant ions based on the mass spectra in Figures 1(a) and (b) and will influence the stoichiometry most. Four measurements were studied, two with each electrode type. These were carefully selected so that we had the same (or extremely similar) apex field between the two sets of NE and GRID analyses making them highly comparable. The average apex fields chosen based on the Ga CSR were $\left(\frac{Ga^{++}}{Ga^{+}} = 0.330 \pm 0.002\ \&\ 0.001 \pm 0.002\right)$ for the NE and $\left(\frac{Ga^{++}}{Ga^{+}} = 0.341 \pm 0.002\ \&\ 0.002 \pm 0.002\right)$ for the GRID electrode. This meant we also had a relatively high and low apex field comparison where the apparent stoichiometry changes by ~30 at.%.

Table I shows a selection of SISCS and mixed double ion hits extracted from the data sets collected using the NE and GRID electrode and for the two apex fields highlighted. The uncertainties quoted are again just the statistical error and were included to highlight which ions are statistically relevant given some of the extremely low counts observed. We also note that although ~500,000 ions for each data set were targeted, a slightly different number of detected

public

events for each data set shown in Table I was found. Thus, although comparing the SISCS and mixed ions from one data set is appropriate, comparing between electrodes or different apex field data sets will suffer a bias due to the number of detected events. To account for this, the number of detected ions making up each data set was included for the determination of the NE:GRID electrode ratio reported in Table I.

For the Ga CSR of 0.330 (NE) and 0.341 (GRID electrode), i.e., highest apex field, we note that the ratio between the SISCS and mixed ions are very similar. If a significant amount of SISCS ion-pile up were occurring, a larger ratio difference for the mixed compared to the SISCS ions would be expected. For the lower apex field data, i.e. Ga CSR = 0.001 (NE) and 0.002 (GRID electrode), the SISCS ion NE:GRID electrode ratio is very similar to that found for the higher apex field. However, an increase for some of the mixed ion pairs where the counts are statistically relevant, e.g., $^{69}Ga^{+}$-$^{14}N_2^{+}$, $^{69}Ga^{+}$-$^{71}Ga^{+}$, $^{69}Ga^{+}$-$^{14}N^{+}$, $^{69}Ga^{+}$-$^{14}N_2^{+}$, would indicate that we now have more co-evaporation. Given that the apparent stoichiometry is the same for both electrodes, then any associated ion pile-up must be either small or not element specific.

Interestingly, the number of multihits (Figure 2(b)) along with the number of ions per pulse (Figure 3) as a function of apex field was shown to increase, but in contrast, the data shown in Table I indicates that the co-evaporation of the ranged ions does not follow the same trend, i.e., increases with field, something that might intuitively have been assumed. If anything, it infers more co-evaporation occurs at a lower apex field. This trend reversal is believed to be related to the data used in the different analyses presented in Figure 2(b), Figure 3 and Table I. For Figures 2(b) and 3, all the ions collected and shown in the mass spectra are included while for Table I, only the ranged peaks are considered. As we increase the apex field, the mass spectrum background increases which is believed to be related to an enhanced DC evaporation [18]. From the double hit

public

data, those coming just from the mass spectrum background can also be isolated, although we cannot attribute a mass to them. Analysis of these background double hits revealed they accounted for ~30 % (NE CSR 0.330) and ~10 % (NE CSR 0.001) of the double hits detected. Likewise for the GRID CSR 0.341 and 0.002 analysis, the background double hits made up ~21 % and ~8 % of the total double hits detected. This indicates that for a higher apex field where the total number of multihits increases a significant fraction of this increase is related to the mass spectrum background. This would therefore explain the inverse trend observed in the results presented in Figures 2(b) and 3 compared to those of Table I.

For the lower apex field where the DC evaporation and background multihits are significantly reduced, the ranged double hits NE:GRID ratio for the two field measurements of Table I indicate an enhanced co-evaporation for the lower field apex field regime. As the parameter varied to change the apex field was the LPE (i.e., tip temperature), then for GaN, this would indicate some sensitivity to the apex temperature over the LPE range applied here. Quantifying the GaN apex temperature, or change in the apex temperature, is far from trivial [29, 30]. However, given the LPE differences, i.e., ΔLPE = 0.005 to 0.5 pJ NE and 0.01 to 3 pJ for the GRID electrode, for the data in Table I, a notable change in the average apex temperature is likely to have occurred. A potential reason for the enhanced co-evaporation at higher tip temperature but lower field may occur due to the following. When an atom field evaporates it leaves an adjacent atom exposed to a higher field, while the more elevated the tip temperature means a lower energy barrier for field evaporation is present. This combination will result in an enhanced probability for co-evaporation. We also note that for the data shown in Table I, the LPE was different between the NE and GRID analysis for similar apex fields, i.e., the LPE was always slightly higher for the GRID analysis to achieve the same apex field. This may be because the evaporation rate between the analyses is not

public

perfectly accounted for in the detection rate compensation approach. As our data would indicate a tip temperature dependence, then the NE to GRID electrode ratio presented will also include a systematic offset. Thus, for the equivalent apex field, the tip temperature of the GRID electrode sample would be higher and therefore suffer more co-evaporation.

public

SISCS ions	NE Ga CSR 0.330	GRID Ga CSR 0.341	Ratio NE:GRID event corrected	NE Ga CSR 0.001	GRID Ga CSR 0.002	Ratio NE:GRID event corrected
$^{69}Ga^{+}$:$^{69}Ga^{+}$	387 ± 20	64 ± 8	5.5 ± 1.0	577 ± 24	56 ± 7	6.8 ± 1.0
$^{69}Ga^{+}$:$^{69}Ga^{++}$	74 ± 9	9 ± 3	7.5 ± 3.0	-	-	-
$^{71}Ga^{+}$:$^{71}Ga^{+}$	138 ± 12	25 ± 5	5 ± 1	253 ± 16	42 ± 6	4 ± 1
$^{71}Ga^{+}$:$^{71}Ga^{++}$	35 ± 6	10 ± 3	3.2 ± 1.0	-	-	-
$^{14}N^{+}$:$^{14}N^{+}$	137 ± 12	25 ± 5	5 ± 1	8 ± 3	1 ± 1	5.3 ± 1.0
$^{14}N_2^{+}$:$^{14}N_2^{+}$	257 ± 16	36 ± 6	6.5 ± 1.0	41 ± 6	4 ± 2	6.8 ± 1.0
Mixed ions	**NE Ga CSR 0.330**	**GRID Ga CSR 0.341**	**Ratio NE:GRID event corrected**	**NE Ga CSR 0.001**	**GRID Ga CSR 0.002**	**Ratio NE:GRID event corrected**
$^{69}Ga^{+}$:$^{14}N_2^{+}$	1337 ± 37	310 ± 18	3.9 ± 0.3	1364 ± 37	43 ± 7	21 ± 5.0
$^{69}Ga^{++}$:$^{14}N_2^{+}$	3261 ± 60	505 ± 22	5.9 ± 0.3	42 ± 6	4 ± 2	6.5 ± 5.0
$^{69}Ga^{+}$:$^{14}N^{+}$	1582 ± 40	280 ± 17	5.2 ± 0.2	220 ± 15	17 ± 4	8.5 ± 3.0
$^{69}Ga^{++}$:$^{14}N^{+}$	9265 ± 96	1165 ± 34	7.3 ± 0.4	40 ± 6	3 ± 2	8.8 ± 8.0
$^{71}Ga^{+}$:$^{14}N_2^{+}$	5936 ± 77	742 ± 27	7.3 ± 0.3	957 ± 31	32 ± 6	20 ± 5
$^{71}Ga^{++}$:$^{14}N_2^{+}$	2025 ± 45	339 ± 18	5.5 ± 0.4	24 ± 5	1 ± 1	16 ± 20
$^{71}Ga^{+}$:$^{14}N^{+}$	965 ± 31	195 ± 14	4.5 ± 0.4	147 ± 12	9 ± 3	11 ± 6
$^{71}Ga^{++}$:$^{14}N^{+}$	815 ± 29	201 ± 14	3.7 ± 0.3	28 ± 5	2 ± 1	9 ± 10
$^{69}Ga^{+}$:$^{69}Ga^{++}$	770 ± 28	193 ± 14	3.6 ± 0.3	33 ± 6	7 ± 3	3.1 ± 2.0
$^{69}Ga^{+}$:$^{71}Ga^{+}$	1012 ± 32	210 ± 15	4.4 ± 0.4	1093 ± 33	85 ± 9	8.5 ± 1.0
$^{69}Ga^{+}$:$^{71}Ga^{++}$	461 ± 21	129 ± 11	4.3 ± 0.3	24 ± 5	3 ± 2	5.3 ± 6.0
$^{69}Ga^{++}$:$^{71}Ga^{+}$	480 ± 22	149 ± 12	2.9 ± 0.3	29 ± 5	3 ± 2	6.4 ± 7.0
$^{69}Ga^{++}$:$^{71}Ga^{++}$	287 ± 17	106 ± 10	2.5 ± 0.3	1 ± 1	1 ± 1	1 ± 1
$^{71}Ga^{+}$:$^{71}Ga^{++}$	323 ± 18	110 ± 10	2.7 ± 0.3	11 ± 3	1 ± 1	7 ± 7
$^{14}N^{+}$:$^{14}N_2^{+}$	584 ± 24	132 ± 11	4.0 ± 0.4	77 ± 9	5 ± 2	10 ± 6

Table I. Selection of GaN same pulse mixed and SISCS double hits measured using the NE and GRID and the ratio between NE and GRID for similar Ga CSR.

public

2. AlN

The second material studied was AlN. Figures 4 (a) and (b) show typical mass spectra taken from an AlN sample analyzed with (a) the CAMECA NE and (b) the GRID electrode. Both spectra show the same mass peaks and are highly representative of what was observed for all the conditions used in the field dependent study conducted. From the spectra the $^{14}N^{++}$, $^{14}N^{+}$, $^{14}N_2{}^{+}$, $^{27}Al^{+}$, $^{27}Al^{++}$ and $^{27}Al^{3+}$ are the most prominent mass peaks found and will therefore have the largest influence on the stoichiometry determined. The mass spectra shown in Figures 4(a) and (b) were also collected under a similar average Al CSR, i.e., $\frac{Al^{++}}{Al^{+}} = 2.47 \pm 0.01$ for the NE and $\frac{Al^{++}}{Al^{+}} = 2.23 \pm 0.01$ for the GRID electrode. As with the GaN, the apparent stoichiometry determined (again 14 Da was assigned to be $^{14}N^{+}$) from the two mass spectra of Figure 4(a) and (b) were also in good agreement, with the NE data yielding Al = 58.8 ± 0.1 at.% and N = 41.2 ± 0.1 at.%; and for the GRID electrode Al = 57.4 ± 0.1 at.% and N = 42.6 ± 0.1 at.%. The errors quoted are again from the 1σ counting statistics only [23].

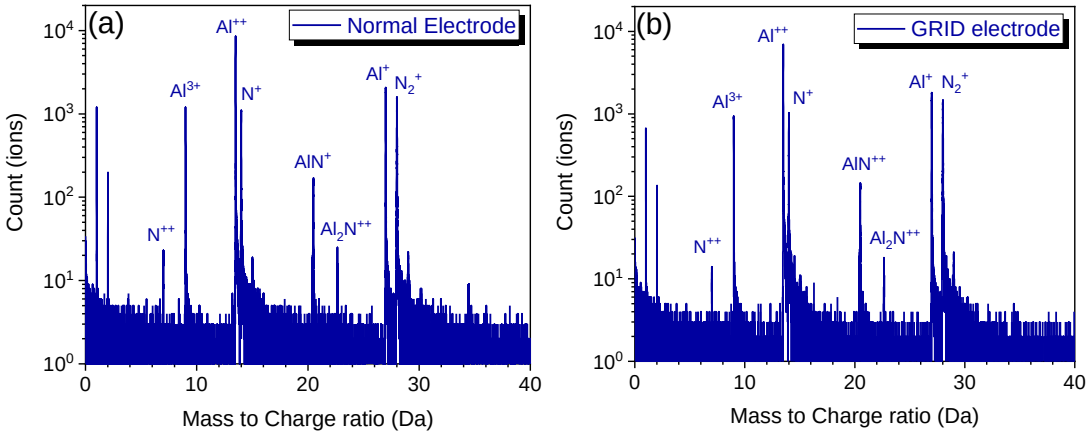

Figure 4. Mass spectra from AlN using (a) the CAMECA NE and (b) the GRID electrode.

public

From a set of field dependent measurements performed on the AlN using the NE and GRID electrode, the apparent stoichiometry as a function of Al CSR, i.e., apex field, determined is shown in Figure 5(a). From Figure 5(a) we observe that the N is always underestimated. This is very different to GaN where the correct stoichiometry was attained for higher apex fields. However, this inability to measure the correct stoichiometry has also been observed for AlGaN when the Al fraction becomes comparable or greater than the amount of Ga present [18]. As seen in Figure 5 (a), the apparent stoichiometry determined using either the NE and GRID electrode again shows excellent agreement although this time we have fewer GRID electrode data points and less of a change in apparent stoichiometry (~5 at.%) with CSR, i.e. apex field.

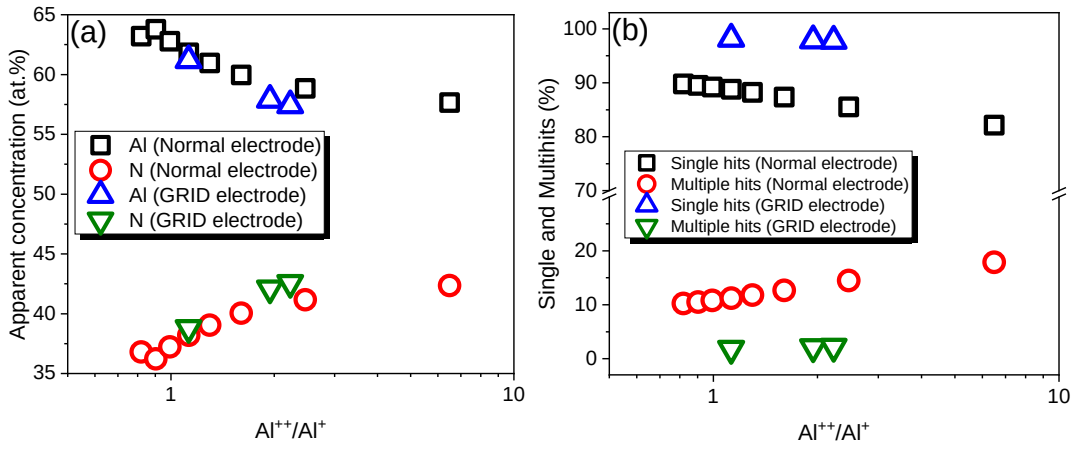

Figure 5. (a) Plot of the apparent Al and N stoichiometry as a function of Al CSR and (b) Single and multihits as a function of Al CSR for the same data set.

From the data, the percentage of single and multihits were extracted and plotted as a function of Al CSR in Figure 5(b). Again, we see a significant difference in the number of detected multihits between the two electrodes used as a function of Al CSR. The GRID electrode multihits are much

public

lower than the NE by a factor of ~4. Even with this significant difference in multihit level, the apparent stoichiometry as a function of apex field remains similar.

From the data the maximum number of ions per pulse detected as function of Al CSR for both the NE and GRID electrode were also determined and are presented in Figure 6. From Figure 6 the number of ions per pulse for the NE is ~2 times more than for the GRID electrode, i.e., ~7 for the NE compared to ~3 for the GRID electrode. These values are comparable to those found for the GaN. Again, the higher number of ions per pulse for the NE compared to the GRID electrode is expected. This reflects the detection efficiency difference between the two electrodes. However, even for the NE the behaviour with field appears invariant this time. This may be due to a smaller change in apex field compared to the GaN. Although we cannot directly measure the apex field, we note the Ga CSR (for the NE GaN analysis) varied by over two orders of magnitude compared to about one here. For the GRID electrode only 3 counts per pulse for the apex field range measured is observed. This is again believed to be the result of the number of multiples generated combined with the lower detection efficiency of the GRID electrode.

As Al is a single isotope element, AlN can be considered as almost being made up of two single isotope elements unlike GaN. Therefore, the probability for same isotope co-evaporation is similar for both species. However, the elements FOE, like GaN, remain significantly different. A value of 19 V/nm is reported [25] for Al (based on pure Al) but again N is not reported. However, applying Müller's image hump model in combination with Equation 1 to find the Al and N energy barrier at zero field using the relevant AlN cohesive energy [27], Al and N ionization energies [25], and the AlN surface work function [31], the FOE for N and Al for the AlN matrix was estimated to be ~200 V/nm and ~50 V/nm respectively. This again supports N as being the element hardest to field evaporate.

public

In a similar way to that carried out on the GaN data, the amount of SISCS and mixed ions detected using both the NE and GRID were again investigated through the number and type of double hit ions per pulse recorded. The double ion combinations explored included $^{27}Al^{1+/2+/3+}$, $^{14}N^{++}$, $^{14}N^{+}$ and $^{14}N_2^{+}$ because these were the most significant ions observed in Figures 4(a) and (b). Six measurements were taken into consideration this time, three with each electrode type. The same (or extremely similar) apex field between the three sets of NE and GRID analyses were again chosen making them highly comparable. The average apex fields based on the Al CSR were $\left(\frac{Al^{++}}{Al^{+}} = 1.127 \pm 0.005\right), \left(\frac{Al^{++}}{Al^{+}} = 1.603 \pm 0.007\right)$ and $\left(\frac{Al^{++}}{Al^{+}} = 2.47 \pm 0.01\right)$ for the NE and $\left(\frac{Al^{++}}{Al^{+}} = 1.126 \pm 0.005\right), \left(\frac{Al^{++}}{Al^{+}} = 1.945 \pm 0.009\right)$ and $\left(\frac{Al^{++}}{Al^{+}} = 2.23 \pm 0.01\right)$ for the GRID electrode. Table II shows a selection of the mixed and SISCS double hit ions extracted from the data collected using the NE and GRID electrode for the three apex fields. The uncertainties quoted are again just the statistical error and were again included to highlight which ions were statistically relevant given some of the extremely low counts observed. Like for the GaN, ~500,000 ions for each data set were targeted but a slightly different number of detected events for each data set was collected. To account for this, the number of detected ions making up each data set was again included for the determination of the NE:GRID electrode ratio reported in Table II.

From Table II we observe that the ratio between NE:GRID electrode for the SISCS and mixed ions regardless of the three apex fields studied remains extremely similar. When we compare the SISCS and mixed ions for each field, a very small difference in the NE:GRID ratio is observed, with the mixed ions showing a slightly higher ratio indicating there may be some co-evaporation. Given the apparent stoichiometry determined between the NE and GRID electrode for each of the three apex fields analyzed were the same; but the apparent stoichiometry with apex field changed

public

by >5 at.%; and the N is always ≥7 at.% underestimated, the similarity between the three field measurements double hit analysis again does not support co-evaporation ion pile-up as the primary cause for the apparent stoichiometric variation with apex field and/or the level of N underestimation.

public

Table II. Selection of AlN mixed and SISCS double hits measured using the NE and GRID and the ratio between NE and GRID for similar Ga CSR.

SISCS ions	**NE** **Al CSR 2.47**	**GRID** **Al CSR 2.23**	**Ratio NE:GRID event corrected**
$^{27}Al^{+}$:$^{27}Al^{+}$	27 ± 5	10 ± 3	2.0 ± 1.0
$^{27}Al^{++}$:$^{27}Al^{++}$	246 ± 16	59 ± 8	3.1 ± 0.6
$^{27}Al^{+++}$:$^{27}Al^{+++}$	2 ± 1	2 ± 1	1 ± 1
$^{14}N^{+}$:$^{14}N^{+}$	119 ± 11	53 ± 7	1.7 ± 0.4
$^{14}N_2^{+}$:$^{14}N_2^{+}$	112 ± 11	31 ± 6	2.7 ± 0.7
Mixed ions	**NE** **Al CSR 2.47**	**GRID** **Al CSR 2.23**	**Ratio NE:GRID event corrected**
$^{27}Al^{+}$:$^{14}N_2^{+}$	1032 ± 32	167 ± 13	4.6 ± 0.5
$^{27}Al^{++}$:$^{14}N_2^{+}$	7849 ± 89	1132 ± 34	5.2 ± 0.2
$^{27}Al^{+++}$:$^{14}N_2^{+}$	635 ± 25	152 ± 12	3.1 ± 0.4
$^{27}Al^{+}$:$^{14}N^{+}$	2226 ± 47	430 ± 21	3.9 ± 0.3
$^{27}Al^{++}$:$^{14}N^{+}$	6290 ± 79	1167 ± 34	4.1 ± 0.2
$^{27}Al^{+++}$:$^{14}N^{+}$	1965 ± 44	456 ± 21	3.2 ± 0.2
$^{27}Al^{+}$:$^{27}Al^{++}$	1348 ± 37	293 ± 17	3.5 ± 0.3
$^{27}Al^{+}$:$^{27}Al^{+++}$	873 ± 30	200 ± 14	3.3 ± 0.3
$^{27}Al^{++}$:$^{27}Al^{+++}$	1761 ± 42	354 ± 14	3.7 ± 0.3
$^{14}N^{+}$:$^{14}N_2^{+}$	847 ± 29	257 ± 16	2.5 ± 0.2

SISCS ions	**NE** **Al CSR 1.603**	**GRID** **Al CSR 1.945**	**Ratio NE:GRID event corrected**
$^{27}Al^{+}$:$^{27}Al^{+}$	43 ± 6	14 ± 4	2.8 ± 0.9
$^{27}Al^{++}$:$^{27}Al^{++}$	282 ± 17	64 ± 8	4.1 ± 0.6
$^{27}Al^{+++}$:$^{27}Al^{+++}$	2 ± 1	1 ± 1	2 ± 2
$^{14}N^{+}$:$^{14}N^{+}$	246 ± 16	114 ± 11	2.0 ± 0.2
$^{14}N_2^{+}$:$^{14}N_2^{+}$	147 ± 12	42 ± 6	3.2 ± 0.6
Mixed ions	**NE** **Al CSR 1.603**	**GRID** **Al CSR 1.945**	**Ratio NE:GRID event corrected**
$^{27}Al^{+}$:$^{14}N_2^{+}$	1331 ± 36	284 ± 17	4.3 ± 0.3

public

$^{27}Al^{++}$:$^{14}N_2^+$	7981 ± 59	1483 ± 39	5.0 ± 0.2
$^{27}Al^{+++}$:$^{14}N_2^+$	602 ± 25	203 ± 14	2.7 ± 0.2
$^{27}Al^{+}$:$^{14}N^+$	2523 ± 50	680 ± 26	3.4 ± 0.2
$^{27}Al^{++}$:$^{14}N^+$	6117 ± 78	1624 ± 40	3.5 ± 0.1
$^{27}Al^{+++}$:$^{14}N^+$	2004 ± 45	634 ± 25	2.9 ± 0.1
$^{27}Al^{+}$:$^{27}Al^{++}$	2037 ± 45	455 ± 21	4.1 ± 0.2
$^{27}Al^{+}$:$^{27}Al^{+++}$	906 ± 30	231 ± 15	3.6 ± 0.3
$^{27}Al^{++}$:$^{27}Al^{+++}$	1714 ± 41	511 ± 23	3.1 ± 0.2
$^{14}N^{+}$:$^{14}N_2^+$	1016 ± 32	410 ± 20	2.3 ± 0.1

SISCS ions	**NE** **Al CSR 1.127**	**GRID** **Al CSR 1.126**	**Ratio NE:GRID event corrected**
$^{27}Al^{+}$:$^{27}Al^{+}$	59 ± 8	31 ± 6	1.7 ± 0.4
$^{27}Al^{++}$:$^{27}Al^{++}$	227 ± 15	77 ± 9	2.7 ± 0.4
$^{27}Al^{+++}$:$^{27}Al^{+++}$	0 ± 0	0 ± 0	0 ± 0
$^{14}N^{+}$:$^{14}N^{+}$	197 ± 14	127 ± 11	1.4 ± 0.2
$^{14}N_2^{+}$:$^{14}N_2^{+}$	120 ± 11	43 ± 7	2.5 ± 0.5
Mixed ions	**NE** **Al CSR 1.127**	**GRID** **Al CSR 1.126**	**Ratio NE:GRID event corrected**
$^{27}Al^{+}$:$^{14}N_2^+$	1162 ± 34	281 ± 17	3.8 ± 0.3
$^{27}Al^{++}$:$^{14}N_2^+$	5589 ± 75	1018 ± 32	5.0 ± 0.2
$^{27}Al^{+++}$:$^{14}N_2^+$	417 ± 20	137 ± 12	2.8 ± 0.3
$^{27}Al^{+}$:$^{14}N^+$	1895 ± 44	569 ± 24	3.0 ± 0.2
$^{27}Al^{++}$:$^{14}N^+$	3932 ± 63	1095 ± 27	3.3 ± 0.1
$^{27}Al^{+++}$:$^{14}N^+$	1182 ± 34	418 ± 20	2.6 ± 0.2
$^{27}Al^{+}$:$^{27}Al^{++}$	2044 ± 45	503 ± 22	3.7 ± 0.2
$^{27}Al^{+}$:$^{27}Al^{+++}$	698 ± 26	223 ± 15	2.9 ± 0.2
$^{27}Al^{++}$:$^{27}Al^{+++}$	1170 ± 34	338 ± 18	3.2 ± 0.2
$^{14}N^{+}$:$^{14}N_2^+$	765 ± 28	366 ± 19	1.9 ± 0.1

Given the findings presented for both the GaN and AlN does not support ion pile-up as the primary loss mechanism behind the field dependent compositional bias, further studies need to be

public

undertaken to find the underlying cause. Similar behavior to GaN/AlN has been shown to occur for oxides, e.g., α-Fe_2O_3 and $SrTiO_3$ [32, 33], but for these samples it was the O that was severely underestimated. A very probable mechanism behind underestimation of elements like N or O in nitrides and oxides is thought to be the formation and emission of neutrals, which cannot be detected. Nevertheless, how these neutrals form remains a topic of debate. Diercks *et al*. [34] made a convincing argument for the loss of nitrogen at higher LPE through N_2 neutrals. Based on the sample's crystal planes, laser orientation and lowering of the decomposing temperature under vacuum, they concluded N is lost through N_2 sublimation. As the loss of N here appears to correlate with higher LPE (tip temperature) and lower apex field based on CSR analysis, thermal sublimation of N/N_2 cannot be ruled out. However, Gault *et al*. [35] somewhat opposed Diercks hypothesis from a theoretical viewpoint. They countered that decomposition of N/N_2 neutrals during an APT experiment was unlikely based on the expected tip temperature. Moreover, they also indicated that if N_2 were to be desorbed from the surface, it would behave like that of an imaging gas in field ion microscopy (FIM) i.e., become ionized, as reported by Suchorski *et al*. [36]. They then went on to propose that the loss of N comes from the field emission of molecular ions that undergo dissociation to form N/N_2 neutrals. They supported their dissociation proposition through a GaN Saxey map [4]. This dissociation hypothesis could also offer a potential explanation to support our findings. As proposed by Gault *et al*. [35], any N/N_2 neutrals formed from the dissociation process will have the ability to ionize during their time of flight. This will also depend on the distance from the apex at which the dissociation occurs and the apex field at this point. Hence, the lower the LPE, the higher the apex field and the greater distance expected from the apex for this neutral ionization to occur. Now, if more of the N/N_2 neutrals arising from dissociation were to ionize with increasing apex field, this could explain the improved composition

public

observed at higher fields. Moreover, for AlN we never reach the correct stoichiometry compared to GaN. A potential reason for this is that the AlN molecules are lighter in mass compared to their GaN equivalents, and so they will exit the high field region closer to the apex quicker. Although this will reduce the opportunity for AlN dissociation to occur, AlN possesses a much larger electric dipole than GaN which compensates this effect [37]. An impact of this quicker exit from the high field region is that any N neutrals formed by dissociation would have less time to ionize. This would lead to a reduced ionization efficiency for the dissociated N neutrals and may be an underlying cause for why we never reach the correct stoichiometry for AlN compared with GaN.

If a lack of ion generation and/or emission were the issue, effort towards developing a better understanding of the field evaporation mechanism is required. Only by determining this for nanometer scale samples that are subjected to high electric fields and laser illumination (i.e., thermal impact), a far from trivial task we note, can the root cause of the compositional bias we so regularly observe in APT with oxides and nitrides be explained. Moreover, such an understanding would aid in the development of the next generation of experimental equipment and/or analysis conditions to minimize/avoid this in the future. It should also be noted that if ions are being lost, e.g., by neutral formation, not only is the composition quantification compromised, but also the spatial resolution of the reconstructed data [38, 39], and this is something APT aims to excel in.

Conclusions

In this paper we have investigated the correlation between field dependent compositional bias with multihits and any associated ion pile-up for nitride materials. In the case of GaN, the lower the apex field the greater the divergence from the correct stoichiometry, while for AlN, the correct stoichiometry was never reached. Several factors were presented, including FOE calculations combined with N being the element always underestimated, which indicate N as having the

public

necessary characteristics for being prone to ion pile-up. Using a CAMECA NE in combination with a GRID electrode specially designed to manipulate the ion pile-up behavior, no impact on the apparent stoichiometry with field was observed. Our findings do not therefore support N ion pile-up as the primary and underlying cause for the field dependent compositional bias observed for GaN and AlN.

Acknowledgments

The authors acknowledge the financial support by FWO Hercules through project ZW13_09.

References

[1] R. Cuduvally, R. J. H. Morris, P. Ferrari, J. Bogdanowicz, C. Fleischmann, D Melkonyan, W. Vandervorst, Potential sources of compositional inaccuracy in the atom probe tomography of $In_xGa_{1-x}As$, Ultramicroscopy 210 (2020) 112918.

[2] Z. Peng, F. Vurpillot, P-P Choi, Y. Li, D. Raabe, B. Gault, On the detection of multiple events in atom probe tomography, Ultramicroscopy 189 (2018) 54–60.

[3] M. Thuvander, A.Kvist, L. J. S. Johnson, J. Weidow, H-O Andrén, Reduction of multiple hits in atom probe tomography, Ultramicroscopy 132 (2013) 81–85.

[4] D. W. Saxey, Correlated ion analysis and the interpretation of atom probe mass spectra, Ultramicroscopy 111 (2011) 474-479.

[5] G. Da Costa, H. Wang, S. Duguay, A. Bostel, D. Blavette, B. Deconihout, Advance in multi-hit detection and quantization in atom probe tomography, Review of Scientific Instruments 83 (2012) 123709.

[6] F. Meisenkothen, E. B. Steel, T. J. Prosa, K. T. Henry, R. P. Kolli, Effects of detector dead-time on quantitative analyses involving boron and multi-hit detection events in atom probe tomography, Ultramicroscopy 159 (2015) 101–111.

[7] G. Da Costa, Chapter 6: Atom Probe Tomography: Detector Issues and Technology, Eds. W. Lefebvre-Ulrikson, F. Vurpillot, X. Sauvage, Atom Probe Tomography: Put Theory into Practice Academic Press, Elsevier Inc, 2016 155-181.

[8] B. Deconihout, F. Vurpillot, M. Bouet, L. Renaud, Improved ion detection efficiency of microchannel plate detectors, Review of Scientific Instruments 73 (2002) 1734-1740.

public

[9] G. Da Costa, F. Vurpillot, A. Bostel, M. Bouet, B. Deconihout, Design of a delay-line position-sensitive detector with improved Performance, Review of Scientific Instruments 76 (2005) 013304.
[10] O. Jagutzki, A. Cerezo, A. Czasch, R. Dörner, M. Hattaß, M. Huang, V. Mergel, U. Spillmann, K. Ullmann-Pfleger, T. Weber, H. Schmidt-Böcking, G. D. W. Smith, Multiple Hit Readout of a Microchannel Plate Detector with a Three-Layer Delay-Line Anode, IEEE Transactions on nuclear science 49 (2002) 2477-2483.
[11] F. De Geuser, B. Gault, A. Bostel, F. Vurpillot, Correlated field evaporation as seen by atom probe tomography, Surface Science 601 (2007) 536–543.
[12] L. Yao, B. Gault, J. M. Cairney, S. P. Ringer, On the multiplicity of field evaporation events in atom probe: a new dimension to the analysis of mass spectra, Philosophical Magazine Letters. 90 (2010) 121–129.
[13] J. Takahashi, K. Kawakami, A quantitative model for preferential evaporation and retention for atom probe tomography, Surface Interface Analysis, 46 (2014) 535-543.
[14] Y. Tu, H. Takamizawa, B. Han, Y. Shimizu, K. Inoue, T. Toyama, F. Yano, A. Nishida, Y. Nagai, Influence of laser power on atom probe tomographic analysis of boron distribution in silicon, Ultramicroscopy 173 (2017) 58-63.
[15] T. Martin, A.J. London, B. Jenkins, S. E. Hopkin, J. O. Douglas, P.D. Styman, P. A. J. Bagot, M. P. Moody, Comparing the consistency of atom probe tomography measurements of small-scale segregation and clustering between the LEAP 3000 and LEAP 5000 instruments, Microsc. Microanal. 23 (2017) 227-237.
[16] L. Mancini, N. Amirifar, D. Shinde, I. Blum, M. Gilbert, A. Vella, F. Vurpillot, W. Lefebvre, R. Lardé, E. Talbot, P. Pareige, X. Portier, A. Ziani, C. Davesnne, C. Durand, J. Eymery, R. Butté, J-F Carlin, N. Grandjean, L. Rigutti, Composition of wide bandgap semiconductor materials and nanostructures measured by atomprobe tomography and its dependence on the surface electric field, J. Phys. Chem. C. 118 (2014) 24136-2416.
[17] D. R. Diercks, B. P. Gorman, Nanoscale measurement of laser-induced temperature rise and field evaporation effects in CdTe and GaN, J. Phys. Chem. C 119 (2015) 20623-20631.
[18] R.J.H. Morris, R. Cuduvally, D. Melkonyan, C. Fleischmann, M. Zhao, L. Arnoldi, P. van der Heide, W. Vandervorst, Toward accurate composition analysis of GaN and AlGaN using atom probe tomography, J. Vac. Sci. Technol. B. 36 (3) (2018) 03F130-1.

public

[19] R.J.H. Morris, R. Cuduvally, D. Melkonyan, M. Zhao, P. van der Heide, W. Vandervorst, Atom probe of GaN/AlGaN heterostructures: the role of electric field, sample crystallography and laser excitation on quantification, Ultramicroscopy 206 (2019) 112813.
[20] M. Zhao, Y. Saripalli, P. K. Kandaswamy, H. Liang, A. Firrincieli, S. Decoutere, E. Vancoille, Growth and characterization of DH-HEMT structures with various AlGaN barriers and AlN interlayers on 200 mm Si(111) substrates, Phys. Status Solidi C. 11,(2014) 446–449.
[21] M. K. Miller, K. F. Russell, K. Thompson, R. Alvis, D. J. Larson, Review of atom probe FIB-based specimen preparation methods, Microsc. Microanal. 13 (6) (2007) 428–436.
[22] Kingham, D. R. The post- ionization of field evaporated ions: a theoretical explanation of multiple charge states. Surf. Sci. 116 (1982) 273–301.
[23] M. K. Miller, R. G. Forbes, Atom Probe Tomography, Materials Characterization 60 (2009) 461-469.
[24] LEAP® 5000 LOCAL ELECTRODE ATOM PROBE PRODUCT DESCRIPTION 30437K – LEAP Product Description.
[25] T. T. Tsong, Field ion image formation, Surface Science 70 (1978) 211-233.
[26] R. G. Forbes, Field evaporation theory: a review of basic ideas, Applied Surface Science 87/88 (1995) 1-11.
[27] M. Fuchs, J. L. F. Da Silva, C. Stampfl,* J. Neugebauer, and M. Scheffler, Cohesive properties of group-III nitrides: A comparative study of all-electron and pseudopotential calculations using the generalized gradient approximation, Physical Review B 65 (2002) 245212.
[28] V. Bougrov, M. E. Levinshtein, S. L. Rumyantsev, A. Zubrilov, in Properties of Advanced Semiconductor Materials GaN, AlN, InN, BN, SiC, SiGe. Eds. M. E. Levinshtein, S. L. Rumyantsev, M. S. Shur, John Wiley & Sons, Inc., New York, 2001, 1-30.
[29] E. A. Marquis, B. Gault, Determination of the tip temperature in laser assisted atom-probe tomography using charge state distributions, Journal of applied Physics, 104 (2009) 084914.
[30] A. Kumar, J. Bogdanowicz, J. Demeulemeester, D. Bran, D. Melkonyan, C. Fleischmann, W. Vandervorst, Measurement of the apex temperature of a nanoscale semiconducting field emitter illuminated by a femtosecond laser pulse, Journal of Applied Physics 124, (2018) 245105.
[31] Y. Goldberg, in Properties of Advanced Semiconductor Materials GaN, AlN, InN, BN, SiC, SiGe. Eds. M. E. Levinshtein, S. L. Rumyantsev, M. S. Shur, John Wiley & Sons, Inc., New York, 2001, 1-47.

public

[32] M. Bachhav, F. Danoix, B. Hannoyer, J. M. Bassat, R. Danoix, Investigation of O-18 enriched hematite (α-Fe_2O_3) by laser assisted atom probe tomography, International Journal of Mass Spectrometry 335 (2013) 57-60.

[33] R. J. H. Morris, M. I. Popovici, J. Meersschaut, J. E. Scheerder, L. Goux, G. S. Kar, C. Fleischmann, W. Vandervorst, P. van der Heide, Stoichiometric analysis of superficial Ba doped Strontium Titanium Oxide layers using APT: the case of the missing Oxygen!, Microscopy and Microanalysis 27(S1) (2021) 2480-2481.

[34] D.R. Diercks, B.P. Gorman, R. Kirchhofer, N. Stanford, K. Bertness, M. Brubaker, Atom probe tomography evaporation behavior of C-axis GaN nanowires: Crystallographic, stoichiometric, and detection efficiency aspects. J. Appl. Phys. 114 (2013) 184903. http://dx.doi.org/10.1063/1.4830023.

[35] B. Gault, D.W. Saxey, M.W. Ashton, S.B. Sinnott, A.N. Chiaramonti, M.P. Moody, D.K. Schreiber, Behavior of molecules and molecular ions near a field emitter, New Journal of Physics. 18 (2016) 033031. http://doi.org/10.1088/1367-2603/18/3/033031

[36] Y. Suchorski, M.K. Medvedev, J.H. Block, Noble-gas-like mechanism of localized field ionization of nitrogen as detected by field ion appearance energy spectroscopy, Appl. Surf. Sci., 94/95 (1996) 217-223.

[37] D. Zanuttini, I. Blum, E. di Russo, L. Rigutti, F. Vurpillot, J. Douady, E. Jacquet, P.-M. Anglade, B. Gervais, Dissociation of GaN_2^+ and AlN_2^+ in APT: Analysis of experimental measurements, J. Chem. Phys 149 (2018) 134311.

[38] B. Gault, D. Haley, F. de Geuser, M. P. Moody, E. A. Marquis, D. J. Larson, B. P. Geiser, Advances in the reconstruction of atom probe tomography data, Ultramicroscopy, 111 (2011) 448-457

[39] F. Vurpillot, B. Gault, B. P. Geiser, D. J. Larson, Reconstructing atom probe data: A review, Ultramicroscopy, 132 (2013) 19-30.

public